Published in final edited form as:
Microvasc Res. 2009 September ; 78(2): 191–198. doi:10.1016/j.mvr.2009.04.001.

NO/Peroxynitrite Dynamics of High Glucose Exposed HUVECs:

Chemiluminescent Measurement & Computational Model

Sunil Potdar and **Mahendra Kavdia***
Biomedical Engineering Program, University of Arkansas, Fayetteville, AR 72701

Abstract

Pathogenesis of many of diabetes-related vascular complications is associated with endothelial cell (EC) dysfunction, which is reduced bioavailability of EC-released nitric oxide (NO). Interaction dynamics of NO, superoxide (O_2^-) and peroxynitrite ($ONOO^-$) are dependent on both their productions and consumptions through various pathways. Quantitative knowledge of these interaction dynamics in high glucose-induced EC dysfunction remains poorly understood. We developed an integrated experimental and computational approach to gain a quantitative understanding of the interactions of NO, O_2^- and $ONOO^-$ in high glucose-exposed ECs. End-products, nitrite and nitrate, were measured using a chemiluminescence analyzer. A computational biochemical reaction network model was developed to predict the effect of high glucose on ECs NO, O_2^- and $ONOO^-$. ECs NO and O_2^- productions increased in high glucose as evidenced by increased total NOx concentration, primarily increasing nitrate concentration. The model predicted an increase in O_2^- and $ONOO^-$ concentrations and a decrease in NO concentration in high glucose conditions. Administration of superoxide dismutase (SOD) decreased O_2^- concentration and increased NO concentration, thus SOD improved high glucose-induced changes in these interactions. An important finding of this study was that the NO bioavailability decreased in high glucose conditions even though NO production of EC increased. The integrated approach provides a framework to predict NO, O_2^- and $ONOO^-$ concentrations and productions that are difficult to measure in one experiment and will be useful in further EC dysfunction studies.

Keywords

Nitric oxide; Peroxynitrite; Biotransport; Reaction Network; Kinetic Modeling; Endothelial Cell

Introduction

Endothelium-derived nitric oxide (NO) is a potent vasodilator through its diffusion and subsequent stimulation of target hemoprotein soluble guanylate cyclase (sGC) in vascular smooth muscle (Furchgott and Jothianandan, 1991; Moncada et al., 1991). A reduction in endothelial dependent vasodilatation is known as endothelial dysfunction (Cai and Harrison, 2000). Hyperglycemia leads to reduction in endothelial dependent vasodilatation (Lash et al., 1999; Title et al., 2000) and oxidative stress related to hyperglycemic conditions is an important

*Corresponding Author: Mahendra Kavdia, Ph.D., Biomedical Engineering Program, University of Arkansas, 223 Engineering Hall, Fayetteville, AR 72701, mkavdia@uark.edu, Telephone: (479) 575-2850, Fax: (479) 575-2846

contributor to many vascular complications in diabetics (Ceriello, 2003; Giugliano et al., 1995).

The primary marker for endothelial dysfunction is reduced bioavailability of NO (Brownlee, 2001; Guerci et al., 2001; Title et al., 2000). An increased generation of reactive oxygen species (ROS), particularly superoxide (O_2^-), has been identified as one of the major causes for diabetes related endothelial dysfunction and loss in NO bioavailablity in diabetes (Brownlee, 2001; Guerci et al., 2001; Guzik et al., 2002b). Sources of O_2^- production in vascular tissue include membrane-bound NADPH oxidases, uncoupled endothelial NOS, xanthine oxidase, and cyclooxygenase (Brownlee, 2001; Guzik et al., 2002b; Rieger et al., 2002). One of the main sources of O_2^- in vascular disease are the membrane-associated NADPH oxidases (Graier et al., 1996; Guzik et al., 2002a; Warnholtz et al., 1999; Williamson et al., 1993).

All vascular cells, including endothelial cells and smooth muscle cells, have antioxidant defense mechanisms. Excessive oxidative stress can deplete or inactivate antioxidant enzymes including SOD, catalase, glutathione reductase and glutathione peroxisdase (Faraci, 2003; Jones et al., 2007). This results in elevation of O_2^- levels that can further deactivate NO. Taken together, the current data imply that an elevation of antioxidant levels such as SOD and catalase in diabetic state may become a successful remedy for diabetes-induced oxidative stress and reduce progression of endothelial dysfunction. Several in vivo and in vitro studies have shown promising results to support this hypothesis (Ulker et al., 2004; Weidig et al., 2004; Zhang et al., 2006).

Oxidative stress caused by hyperglycemia plays a key role in the pathogenesis of vascular complications (Brownlee, 2001; Ceriello, 2003; Guzik et al., 2002a). Hyperglycemia has been shown to play a principal role in endothelial cell damage and the control of glucose level delays the onset and progression of vascular complications. In endothelial cells, high glucose is shown to a) upregulate eNOS and NO release with a marked concomitant increase of O_2^- production (Cosentino et al., 1997) and b) increase mitochondrial O_2^- and H_2O_2 (Quijano et al., 2007). The mitochondrial oxidants can activate formation of advanced glycation end products (AGEs), protein kinase C (PKC), and nuclear factor-κB (NF-κB) (Du et al., 2003; Garcia Soriano et al., 2001). Additionally, the $p66^{Shc}$ adaptor protein has been shown to participate in mitochondrial ROS production, by serving as a redox-sensitive enzyme that oxidizes cytochrome *c*, in response to high glucose concentration (Camici et al., 2007; Cosentino et al., 2008).

Thus, the delicate balance between NO and O_2^-, and their interaction product $ONOO^-$ has a key role in diabetes induced vascular complications (Kavdia, 2006; Kojda and Harrison, 1999). The underlying interaction dynamics of NO, O_2^- and $ONOO^-$ are dependent on both their productions as well as consumptions through various pathways. A quantitative knowledge of these interaction dynamics is important for understanding the mechanism of endothelial cell dysfunction and remains poorly understood in high glucose-induced endothelial cell dysfunction. The reasons for this lack of understanding are: a). peroxynitrite can not be detected in situ at present (Yang et al., 2008), b) fluorescence imaging of O_2^- and NO with dihydroethidine (DHE) and diaminofluorescein (DAF), respectively can only provide qualitative information of respective concentration but can not provide qualitative or quantitative information of respective production (Takahama et al., 2006; Zielonka et al., 2008) and c). information of all of these complex interactions can not be obtained in one experiment.

In this study, we developed an integrated experimental and computational approach to study the interactions of NO, O_2^- and $ONOO^-$ in high glucose-exposed endothelial cells. End-products of NO, O_2^- and $ONOO^-$ interactions, nitrite and nitrate, were measured using a

chemiluminescence analyzer and a computational biochemical reaction network model was developed to predict the effect of high glucose on endothelial NO, O_2^- and $ONOO^-$ productions and concentrations. Role of antioxidants, including SOD and α-tocopherol, was also evaluated on these interactions.

Materials and Methods

Materials

Cryopreserved primary human umbilical vein endothelial cells (HUVEC) (Lonza, Rockland, ME) were grown in complete endothelial growth medium (EGM-2, 5.5 mM glucose) supplemented with Bullet kit® (Lonza, Rockland, ME) containing fetal bovine serum, nutrients and hormones. The endothelial cells were grown at 37°C in a humidified 5% CO_2 & 95% air incubator. Endothelial cells were trypsinized upon confluence and plated on a 0.2% gelatin coated glass slide.

Dulbecco's modified eagle's medium (DMEM, 1000 mg/l glucose), D-(+)-glucose, SOD from bovine erythrocytes, and (±)-α- tocopherol were obtained from Sigma (St. Louis, MO). Chemicals for measurements of nitrite and total NOx including, sodium iodide (NaI, ACS grade), sodium nitrate ($NaNO_3$, ACS grade), sodium nitrite ($NaNO_2$, ACS grade), vanadium (III) chloride (VCl_3), and sodium hydroxide (NaOH, ACS grade) were purchased from Sigma (St. Louis, MO). Glacial acetic acid (ACS grade) and hydrochloric acid (HCl, ACS grade) were purchased from VWR international (Suwanne, GA).

Experimental system and protocol

The experiments were carried out using a parallel plate flow chamber (Cytodyne, La Jolla, CA). The glass slide confluent with an endothelial cell monolayer was inverted over the parallel plate flow chamber, and clamped. Prior to mounting on the parallel plate flow chamber, the endothelial cell monolayer on the glass slide was washed 3 times with DMEM to remove build up of nitrite and nitrate over cells. Using a syringe pump (KdScientific, Holliston, MA), DMEM was passed through the flow chamber creating shear stress on endothelial cells. For all experiments, wall shear stress was 1.20 dyn/cm^2. The wall shear stress on endothelial cells can be calculated using a momentum balance for a Newtonian fluid and assuming parallel plate geometry: $\tau = 6Q\mu / bh^2$; where Q is flow rate (0.025 cm^3/s); μ is the viscosity (0.01 dyn s/cm^2); h is the channel height (0.0254 cm); b is the slit width (2 cm); and τ is the wall shear stress. The volume of the flow chamber was 0.381 cm^3. The residence time of solution in chamber was 15.24 sec for a flow rate of 0.025 cm^3/s. Thus, the chamber volume was replenished 4 times every min.

To study the effect of high glucose on endothelial cell NO and O_2^- production, media containing normal glucose DMEM, high glucose DMEM alone or in combination with 100 units/ml SOD (1.13 μM) or 100 μM α-tocopherol were used. The exposure to high glucose and SOD and α-tocopherol was only for the duration of flow experiments. Thus, the glucose changes in this study were acute and may not reflect more chronic conditions.

Nitrite, and total NOx measurements

We assumed the free NO in the collected samples was negligible because all NO generated from the endothelial cells would be converted to its final products, nitrite and nitrate, considering the fast reaction rate of NO with O_2 and O_2^-. Nitrite and total NOx (NO_2^- + NO_3^-) were analyzed using a chemiluminescence analyzer (Model NOA 280i, Seivers, Boulder, CO) (Marwali et al., 2007). This is the most sensitive method for the measurement of nitrite and total NOx in gas/liquid samples. Nitrite and nitrate are the end-products of NO and O_2 or O_2^- interactions. Nitrate concentration was obtained by subtracting nitrite

concentration from total NOx concentration. Aqueous samples of exiting media were collected during the experiments. Using a gas tight syringe (Hamilton, Reno, NV), a volume of 250 μl was injected into a respective reducing solution in a radical purge vessel (Seivers, Boulder, CO). The reducing agent converts nitrite or total NOx from injected samples to NO. The nitrite reducing solution was 0.2 M potassium iodide and glacial acetic acid mixed in a 1:3 (v/v). The total NOx reducing solution was a saturated solution of VCl_3 in HCl (stock solution of 0.8 gm VCl_3 and 8 ml HCL diluted to 100 ml in deionized water) at 95 °C. The reducing solution was continuously bubbled with N_2 to purge NO from the solution and transport NO into the chemiluminescence detector flow cell wherein it reacts with ozone and emits light in the infrared region. Concentrations were obtained using $NaNO_2$ or $NaNO_3$ standard calibration curves. We found a concentration range of 10 nM of nitrite and 50 nM of total NOx to be repeatable with confidence.

All reported concentrations were a net increase in levels of nitrite, nitrate and total NOx obtained by subtracting a concentration from the background concentration of the respective medium. In all the results, sample time points 1, 2, 3, 4, 5, 6 indicate concentration of species in the exiting media collected between 0-1, 1-2, 2-3, 3-4, 4-5, 5-6 min, respectively after onset of shear stress at time 0. Initially, we collected samples at every min for 30 min and measured nitrite and total NOx. After six minutes, there was not much change in the measured values (data not shown). To minimize the subsequent measurements, we collected three samples for the time between 6 and 30 min. Sample time points 7-10, 11-20 and 21-30 indicate average concentration of species in the exiting media collected between 7-10, 11-20, and 21-30 min, respectively.

Production of NO from endothelial cells

The NO production from endothelial cells was calculated from the formula total NOx concentration × volumetric flow rate/surface area of cells. The surface area of cells exposed to shear stress was (15 cm^2).

Computational model description for predictions of O_2^-production and NO, O_2^- and $ONOO^-$ concentrations

The experimental total NO production, and reaction kinetics was utilized to predict O_2^-production and NO, O_2^- and $ONOO^-$ steady-state concentrations within the experimental system. The major reactions in the experimental set up are discussed next.

Autooxidation of NO—In a perfectly mixed aqueous medium, NO oxidizes to form NO_2^- as the final product. This reaction is reported to be third order (first order with O_2 and second order with NO). The overall rate of the reaction is controlled by Eq. (1) (Lewis and Deen, 1994).

$$2NO+O_2 \xrightarrow{k_1} 2NO_2, \tag{1}$$

$$NO_2+NO \underset{k_{-2}}{\overset{k_2}{\longleftrightarrow}} N_2O_3, \tag{2}$$

$$N_2O_3+H_2O \xrightarrow{k_3} 2NO_2^-+2H^+, \tag{3}$$

Combining Eqs. 1-3 results in an overall reaction of NO autooxidation i.e. $4NO+O_2 2H_2O \rightarrow 4NO_2^-+4H^+$, thus 4 NO molecules are oxidized by 1 O_2 molecule, such that the nitrite formation is four times the rate of reaction (k_1) in Eq 1.

Reaction of NO with O_2^-—Eq. (4) represents reaction of NO with O_2^-. This is the most rapid reaction of NO. The product of this reaction is $ONOO^-$, which is assumed to be in rapid equilibrium with the protonated form peroxynitrous acid (ONOOH). Finally, ONOOH decomposes to form NO_2^- and NO_3^- as shown by Eqs. (5) and (6) respectively (Koppenol et al., 1992;Pfeiffer et al., 1997). The total peroxynitrite formed from NO and superoxide reaction is represented as C_{PER}.

$$NO+O_2^- \xrightarrow{k_4} ONOO^- \leftrightarrow ONOOH, \tag{4}$$

$$ONOOH \xrightarrow{k_5} NO_3^-+H^+, \tag{5}$$

$$ONOOH \xrightarrow{k_6} NO_2^-+\frac{1}{2}O_2+H^+, \tag{6}$$

Dismutation of superoxide—SOD catalyzes conversion of O_2^- to hydrogen peroxide (H_2O_2) and molecular oxygen. The reaction rate constant of scavenging of O_2^- by SOD is three times lower than the reaction rate constant of NO and O_2^-. The extent of NO reaction with O_2^- is limited by scavenging of O_2^- by SOD (Fridovich, 1995). Therefore, the amount of O_2^- reacting with NO would be that escaped by SOD scavenging reaction.

$$O_2^- H_2O \xrightarrow{SOD,k_7} \frac{1}{2}O_2+\frac{1}{2}H_2O_2+OH^-, \tag{7}$$

Other important reactions—NO_2^- formation can also occur via Eq. (8) with NO reacting with $ONOO^-$ or ONOOH (Pfeiffer et al., 1997). The spontaneous dismutation of O_2^- to hydrogen peroxide is represented by Eq. (9) (Fridovich, 1995). The carbon dioxide (CO_2) catalyzed conversion of $ONOO^-$ to NO_3^- is shown by Eq. (10) (Uppu et al., 1996). Also, α-tocopherol (at) can scavenge the O_2^- anion with a second-order rate constant of 4.5×10^3 $M^{-1}s^{-1}$ (Gotoh and Niki, 1992). Other forms of vitamin E could have different rate constants that can be incorporated by modifying the last term on the right hand side of Equation 13.

$$ONOO^- (ONOOH)+NO \xrightarrow{k_g} NO_2+NO_2^-, \tag{8}$$

$$HO_2+O_2^-+H_2O \xrightarrow{k_9} O_2+H_2O_2+OH^-, \tag{9}$$

$$ONOO^-+CO_2+H_2O \xrightarrow{k_{10}} NO_3^-+CO_3^{2-}+2H^+, \tag{10}$$

Model equations

The mass balance equations for NO_2^-, NO_3^-, and O_2^- and total peroxynitrite (sum of C_{ONOO^-} and C_{ONOOH}) assuming a steady-state for O_2^- and total peroxynitrite ($dC_i/dt \approx 0$) are

$$\frac{dC_{NO_2^-}}{dt} = 4k_1 C_{NO}^2 C_{o_2} + 3k_8 C_{NO} C_{PER} + k_6 C_{ONOOH}, \tag{11}$$

$$\frac{dC_{NO_3^-}}{dt} = k_5 C_{ONOOH} + k_{10} C_{CO_2} C_{ONOO^-}, \tag{12}$$

$$\frac{dC_{O_2^-}}{dt} = 0 = S_{O_2^-} - k_4 C_{NO} C_{o_2^-} - k_7 C_{SOD} C_{o_2^-} - k_9 C_{HO_2} C_{o_2^-} - k_{11} C_{at} C_{o_2^-}, \tag{13}$$

$$\frac{dC_{PER}}{dt} = 0 = k_4 C_{NO} C_{o_2^-} - (k_5 + k_6) C_{ONOOH} - k_8 C_{NO} C_{PER} - k_{10} C_{CO_2} C_{ONOO^-}, \tag{14}$$

where $k_1 = 2.4\times10^6$ $M^{-2}s^{-1}$, $k_4 = 6.7\times10^9$ $M^{-1}s^{-1}$, $k_5 = 3.1$ s^{-1}, $k_6 = 1.4$ s^{-1}, $k_7 = 1.6\times10^9$ $M^{-1}s^{-1}$, $k_8 = 9.1\times10^4$ $M^{-1}s^{-1}$, $k_9 = 8.0\times10^7$ $M^{-1}s^{-1}$, $k_{10} = 5.8\times10^4$ $M^{-1}s^{-1}$, $k_{11} = 4.5\times10^3$ $M^{-1}s^{-1}$ (Chen et al., 1998; Gotoh and Niki, 1992; Kavdia, 2006; Kavdia et al., 2000; Radi, 1998). The rates were further simplified assuming rapid equilibrium for $ONOO^-$/ONOOH and O_2^-/HO_2 occurs such that (C_{ONOOH}/C_{ONOO^-}) = 0.22 and $\left(C_{HO_2}/C_{O_2^-}\right) = 0.0025$ (Chen et al., 1998; Kavdia et al., 2000). For all experiments, the O_2 concentration was assumed to be 210 μM and the aqueous CO_2 concentration was assumed to be 1.1 mM (Kavdia et al., 2000).

From the experimental measurements of NO_2^- and NO_3^- formation ($dC_{NO_2^-}/dt$ and $dC_{NO_3^-}/dt$, respectively), the system of simultaneous equations 11-14 was solved using MatLab. The NO, O_2^-, and $ONOO^-$ concentrations and the O_2^- production $\left(S_{O_2^-}\right)$ were predicted.

Statistics

Total NOx, nitrite and nitrate values from each treatment and at each time point were reported as mean ± SE of n=6 independent experiments. A paired two sample mean t-test was used to determine significant differences between treatments (normal glucose and high glucose; high glucose, and high glucose-SOD or high glucose-α-tocopherol). *P* values < 0.05 were considered significant.

Results

Total NOx concentration dynamics of the endothelial cell in high glucose conditions

To determine the effect of high glucose on endothelial cell NO production, the total NOx concentrations in the exiting media with respect to time were measured for normal glucose (NG, 1000 mg/l) and high glucose (HG, 4500 mg/l) conditions. The total NOx concentrations in the exiting media with respect to time are shown in Figure 1A. The total NOx concentration was 714 ± 91 nM at 1 minute in the normal glucose experiments. The total NOx concentrations

were reduced to 269 ± 87 and 121 ± 57 nM at 2 and 6 min, respectively. The average total NOx concentration of 235 ± 66 nM was observed for 7-30 min.

At all of the time points, the total NOx concentrations were significantly higher ($p<0.05$) in the high glucose experiments than those in the normal glucose experiments. The total NOx concentrations were 1565 ± 230, 586 ± 83, 368 ± 113 and 615 ± 71 for 1, 2, 6 and 7-30 min, respectively in the high glucose experiments. Thus, the total NOx concentrations were 2-3 fold higher in the high glucose experiments than that of the normal glucose experiments.

Differential contributions of total NOx constituents, nitrite and nitrate, in normal and high glucose conditions

The total NOx concentration comprises of nitrite and nitrate, and the concentration profiles of nitrite and nitrate are shown in Figures 1B and 1C, respectively. The contribution of nitrate to total NOx was in the range of 80 to 90% for most of the time points. Additionally, the majority of increased total NOx in the high glucose experiments produced nitrate. For all of the time points, the exiting media nitrate concentrations were significantly higher in the high glucose experiments than that of the normal glucose experiments. The highest concentrations of the exit media nitrite and nitrate were 134 ± 26 and 580 ± 96 nM, respectively in the normal glucose experiments and 151 ± 31 and 1413 ± 208 nM, respectively in the high glucose experiments; these concentrations occurred at 1 min. Though the nitrite concentrations were higher in the high glucose experiments compared to that of the normal glucose experiments except for the 6^{th} minute, the nitrite concentration differences were statistically insignificant.

Effects of SOD and α-tocopherol presence on total NOx, nitrite and nitrate dynamics

The administration of antioxidants, including SOD and α-tocopherol, is a potential therapy for endothelial cell dysfunction. Thus, we studied the effect of the presence of SOD and α-tocopherol on total NOx, nitrite and nitrate dynamics in high glucose conditions. For this purpose, the endothelial cells were exposed to DMEM containing high glucose with SOD (100 units/ml) and α-tocopherol (100 μM). Figures 2A-C show the exiting media concentration profiles for the total NOx, nitrite and nitrate, respectively. As seen in Figure 2A, the presence of SOD or α-tocopherol significantly reduced ($p<0.05$) the total NOx concentrations for all of the time points than that of in the high glucose experiments. For 1, 2, 6 and 7-30 min, the total NOx concentrations were 749 ± 126, 279 ± 107, 160 ± 53 and 223 ± 88, respectively in the SOD experiments and were 670 ± 85, 179 ± 34, 183 ± 115 and 150 ± 73, respectively in the α-tocopherol experiments. The exiting media total NOx concentrations were reduced greater than 40% for all time points in the SOD and α-tocopherol experiments than that of the high glucose experiments.

The nitrite concentrations in the SOD experiments were similar to or higher than that of nitrite concentrations in the high glucose experiments except for the first three time points (Figure 2B). On the other hand, the nitrite concentrations in the α-tocopherol experiments were significantly lower than that of the high glucose experiments for all of the time points. For 1, 2, 6 and 7-30 min, the nitrite concentrations were 94 ± 12, 38 ± 8, 35 ± 13, and 28 ± 12, respectively in the SOD and were 106 ± 17, 17 ± 6, 16 ± 10 and 11 ± 5, respectively in the α-tocopherol.

The nitrate concentrations (Figure 2C) followed similar trends as the total NOx concentrations. SOD and α-tocopherol resulted in significant reduction ($p<0.05$) of nitrate concentrations as compared to the nitrate concentrations in the high glucose experiments. For 1, 2, 6 and 7-30 min, the nitrate concentrations were 655 ± 132, 241 ± 108, 124 ± 49 and 195 ± 91, respectively in the SOD experiments and were 564 ± 83, 162 ± 38, 149 ± 88 and 151 ± 73, respectively in the α-tocopherol experiments.

NO production increases in high glucose conditions

The NO production from endothelial cells was calculated from the total NOx concentration in the exiting media, the media flow rate, and the surface area of cells exposed to shear stress. Note that, each of the time points (but not the slope of the concentration profiles) of total NOx concentrations represents a release rate. This is because of a constant flow rate and single pass of the culture media over the endothelial cells. The NO production was 1.19 pmol s^{-1} cm^{-2} at 1 min in normal glucose. The NO productions reduced to 0.45 and 0.20 pmol s^{-1} cm^{-2} at 2 and 6 min, respectively. The NO production increased to 0.39 pmol s^{-1} cm^{-2} (an average value for 7 - 30 min) for the remainder. Thus, the NO release showed a triphasic pattern; an initial high NO production for the first 3 min, a plateau phase from 3-6 min, and a subsequent sustained NO release. The triphasic patterns of NO production by endothelial cells were observed in all of the experiments as reported in Table 1.

The NO productions increased 2-3 fold in the high glucose experiments as compared to that of the normal glucose experiments. The NO productions in the α-tocopherol experiments reduced below that of in the normal glucose experiments except for the 6 min time point. The NO productions in the SOD experiments also reduced but were similar to that of the normal glucose experiments.

Predictions of O_2^- production and NO, O_2^- and $ONOO^-$ concentrations using mathematical model

Using the mathematical model described by equations 11-14 and the concentrations of nitrite and nitrate, we predicted the O_2^- production and the NO, O_2^-, and $ONOO^-$ concentrations in these experiments. The predicted O_2^- production is presented in Table 1 and the predicted NO, O_2^- and $ONOO^-$ concentrations are shown in Figures 3A-C, respectively.

The O_2^- production from endothelial cells in pmol s^{-1} cm^{-2} unit (Table 1) was calculated from the predicted O_2^- production $\left(S_{O_2^-}\right)$ from the model Equation 13, the media flow rate, and the surface area of cells exposed to shear stress. The O_2^- productions increased 2.3-7.3 fold in the high glucose experiments as compared to that of in the normal glucose experiments. The O_2^- productions in the α-tocopherol experiments were reduced below that of the normal glucose experiments except for the 6 min. The O_2^- productions in the SOD experiments were 1.2-1.5 fold that of the normal glucose experiments.

Though the NO productions increased in the high glucose conditions (Table 1), the NO concentrations reduced in the high glucose experiments due to an increase in the O_2^- productions and O_2^- concentrations. In the normal glucose experiments, NO concentrations were 1.80, 1.05, 0.63 and 0.76 μM, O_2^- concentrations were 3.96, 2.67, 1.74 and 2.47 pM, and $ONOO^-$ concentrations were 0.72, 0.29, 0.14 and 0.26 nM at 1, 2, 6 and 7-30 min, respectively. The NO concentrations decreased 7.6, 3.5, 87.1 and 52.2%, whereas the O_2^- concentrations increased 120, 1109, 54417 and 8504%, and the $ONOO^-$ concentrations increased 143, 132, 523 and 239% at 1, 2, 6 and 7-30 min, respectively in the high glucose experiments as compared to that of the normal glucose experiments. These predictions indicate that the availability of NO significantly decreased whereas the availability of O_2^- and $ONOO^-$ significantly increased in the high glucose experiments as compared to that of the normal glucose experiments.

The NO concentrations decreased 9.5, 39.4, 3.3 and 54.5%, and the O_2^- concentrations changed - 10.0, 12.7, 1222 and 464% at 1, 2, 6 and 7-30 min, respectively in the α-tocopherol experiments as compared to that of in the normal glucose experiments. The $ONOO^-$ concentrations decreased 2.7, 29.7 and 229% at 1, 2, and 7-30 min, respectively but increased 97% at 6 min in the α-tocopherol experiments as compared to that of the normal glucose experiments. These predictions indicate that the availability of NO decreased whereas the

availability of O_2^- increased in the α-tocopherol experiments as compared to that of in the normal glucose experiments.

The concentration changes were -18.5, -12.1, 56.2 and 8.6% for NO, -25.2, 53.9, -21.3 and 10.2 % for O_2^-, and 13.1, 9.1, 10.9 and 1.3% for $ONOO^-$ at 1, 2, 6 and 7-30 min, respectively in the SOD experiments as compared to that of the normal glucose experiments. These predictions indicate that availability of NO increased and O_2^- and $ONOO^-$ decreased for time greater than 7 min in the SOD experiments as compared to that of in the normal glucose experiments.

Discussion

In this study, we investigated the interactions of NO, O_2^- and $ONOO^-$ in high glucose conditions using an integrated experimental and modeling approach. An important finding of this study was that the NO bioavailability decreased in high glucose conditions even though NO production of EC's increased. The integrated approach provides a framework to predict NO, O_2^- and $ONOO^-$ concentrations and productions that are difficult to measure in one experiment and will be useful in further EC dysfunction studies.

Interpretation of nitrite and nitrite concentrations and predicted NO, O_2^- and $ONOO^-$-concentrations

NO reacts very rapidly with superoxide to form the strong oxidant peroxynitrite ($ONOO^-$). The reaction rate constant of superoxide with NO ($k=6.7 \times 10^9\ M^{-1}\ s^{-1}$) to form $ONOO^-$ is 3-6 times higher than with SOD ($k=1.6 \times 10^9\ M^{-1}\ s^{-1}$) to form H_2O_2. To obtain an understanding of the actual reaction rates for a given condition, one can multiply the factor 3-6 with ratio of NO to SOD concentrations. For a constant O_2^-concentration in this study, the reaction rates were $12 \times 10^3\ s^{-1}$ and $0.54 \times 10^3\ s^{-1}$ for the maximum and minimum NO concentrations, respectively, whereas the reaction rate for SOD was $1.80 \times 10^3\ s^{-1}$. The major end-products of NO interactions with molecular oxygen and O_2^- are nitrite (NO_2^-) and nitrate (NO_3^-), respectively. The total NOx is the sum of nitrite and nitrate in a sample. Measurement of nitrite and nitrate/total NOx using the chemiluminescence method can be used to determine NO and O_2^- release by cells (Jones et al., 2008; Marwali et al., 2007; Nalwaya and Deen, 2005).

Based on total NOx concentration, nitrite and nitrate formation rates from experimental measurements, a reaction network model was developed to predict NO and O_2^- productions from endothelial cells. A similar integrated approach of experimental measurements in conjunction with a computational reaction network model of NO, O_2^- and $ONOO^-$ interactions has been used successfully by several studies (Chen and Deen, 2001; Kavdia et al., 2000; Yang et al., 2008). NO reacts readily with O_2 and O_2 derived free radicals. The oxidation of NO by O_2 leads to nitrite formation via the intermediates nitrogen dioxide and nitrous anhydride (Lewis et al., 1995). Under physiological and pathophysiological conditions, O_2^- is generated by a variety of sources including NADPH oxidase, xanthine oxidase, NOS and mitochondrial electron transport chain. Excessive O_2^- production has been associated with a variety of disease conditions including diabetes mellitus, atherosclerosis and hypertension (Cai and Harrison, 2000). NO reacts rapidly with O_2^- to form $ONOO^-$, which is in equilibrium with its protonated form peroxynitrous acid. Peroxynitrous acid decays spontaneously to nitrate (Chen and Deen, 2001). $ONOO^-$ also reacts with NO to form nitrite (Pfeiffer et al., 1997). However, the formation of nitrite is very slow in this pathway to affect the relative amounts of nitrite and nitrate (Chen et al., 1998). The endothelial NO production varied between 0.20-2.61 pmol $s^{-1}\ cm^{-2}$ in this study, which is similar to reported NO production of 0.03-0.68 pmol $s^{-1}\ cm^{-2}$ (Chen and Popel, 2006).

The predictions of NO concentration in this study are representative of this experimental system. In arteriolar blood vessels, we and others have modeled NO biotransport to provide estimates of NO concentration from endothelial NOS and/or neuronal NOS (Kavdia and Popel, 2003; Kavdia and Popel, 2006; Lamkin-Kennard et al., 2003; Vaughn et al., 1998). Additionally, red blood cells are proposed a) to be the major intravascular site of nitrite reduction and storage (Gladwin and Kim-Shapiro, 2008), and b) to contain a NO synthase (Ozuyaman et al., 2008). Thus in vivo NO concentration can be further modulated by red blood cells.

At given production rates of NO and superoxide per area of endothelial cells, the steady-state concentrations of NO and other intermediates depend on the ratio of vascular volume to area. The values calculated in this study are valid for the geometry of the flow cell used, where the ratio volume to area is equal to height = 0.0254 cm. This would correspond to a cylindrical vessel with a diameter of 4 h = 0.1 cm. We performed the simulations for two vessel diameters (data not shown). As the vessels diameters were reduced, accumulation of NO and other intermediates yielded higher concentrations. Additionally, general trends remained similar for cylindrical vessel including a). SOD increased NO levels and decreased superoxide levels and b). α-tocopherol decreased NO levels and increased superoxide levels. A systematic evaluation of parameters including NO and superoxide release for cylindrical geometry is needed and beyond the scope of this manuscript.

Effect of high glucose on endothelial cell production of NO, O_2^- and $ONOO^-$

Our results showed that total NOx and nitrate concentration significantly ($p<0.05$) increased in high glucose as compared to that of in normal glucose. Interestingly, the contribution of nitrate in total NOx increased from 87% (average) in normal glucose to 92% (average) in high glucose. Even though the measured total NOx concentrations significantly increased in high glucose, the predicted NO concentration reduced. The reduction in NO concentration can be attributed to an increase in O_2^- production and concentration. This resulted in higher $ONOO^-$ concentration and results in a shift of NO metabolism towards nitrate. Thus, the results indicate that increased O_2^-production from endothelial cells is responsible for reduction in NO bioavailability in high glucose condition. This is also supported from the restored NO concentrations in SOD conditions.

Effect of antioxidants on high glucose-induced endothelial cell productions and concentrations of NO, O_2^- and $ONOO^-$

The presence of antioxidants play an important role in modulation of oxidative stress and administration of SOD and overexpression of the SOD protein is a potential therapy to treat many disease conditions including hypoxic/ischemic cerebral injury, alzheimer's disease, parkinson's disease, stroke, ischemia-reperfusion injury and diabetes mellitus (Di Filippo et al., 2004; Nishikawa et al., 2000; Stralin and Marklund, 2001).

SOD is one of the most commonly used scavengers of O_2^-. SOD can effectively compete with NO for O_2^- with a rate constant of $1.6 \times 10^9\ M^{-1}\ S^{-1}$ and reduce O_2^- concentration. We observed that the total NOx and nitrate concentrations significantly ($p<0.05$) decreased in SOD as compared to that of in high glucose treatment. Additionally, the endothelial cell NO and O_2^- productions and O_2^- concentration decreased whereas NO concentration increased in SOD as compared to that of in high glucose. The predicted reduction in O_2^- concentration and improvement in NO bioavailabilty in the presence of SOD are consistent with the literature. SOD administration has been shown to improve NO dependent relaxation (Fennell et al., 2002; Maczewski et al., 2004) whereas SOD inhibition has been shown to attenuate NO dependent relaxation (Didion et al., 2002; Lynch et al., 1997).

The nitrate and total NOx concentrations also significantly decreased ($p<0.05$) in α-tocopherol as compared to that of in high glucose. The O_2^- concentrations were similar and NO concentrations decreased concentration for 7-30 min in α-tocopherol as compared to that of in high glucose. Both NO and O_2^- productions and $ONOO^-$ concentration decreased in α-tocopherol as compared to that of in high glucose. This reduction in the overall ability of endothelial cells production of NO might potentially explain contradictory results obtained in α-tocopherol supplementation studies. Researchers reported a positive effect of α-tocopherol on endothelial function (Kinlay et al., 2004; Neunteufl et al., 2000) in animal models, whereas Giardino et al. (Giardino et al., 1996) reported no improvement in NO bioavailability in endothelial cells in α-tocopherol studies. Economides et al. (Economides et al., 2005) also reported α-tocopherol supplementation had no improvement in endothelial function and a worsening of endothelial function with high doses of α-tocopherol in diabetic patients.

Conclusion

The present study demonstrates that endothelial cell NO and O_2^- productions increased in high glucose conditions as evidenced by increased concentrations of total NOx and increased nitrate concentrations being the major contributor. The computational model predicted an increase in O_2^- and $ONOO^-$ concentrations and a decrease in NO concentration in high glucose conditions. Administration of superoxide dismutase decreased O_2^- concentration and increased NO concentration, thus SOD improved high glucose-induced changes in these interactions. The integrated approach presented in this study provides a framework to predict NO, O_2^- and $ONOO^-$ concentrations and productions that are difficult to measure in one experiment and will be useful in further EC dysfunction studies.

Acknowledgement

This work is supported by Arkansas Biosciences Institute, AHA grant 0530050N and NIH grant R01 HL084337.

References

Brownlee M. Biochemistry and molecular cell biology of diabetic complications. Nature 2001;414:813–20. [PubMed: 11742414]

Cai H, Harrison DG. Endothelial dysfunction in cardiovascular diseases: the role of oxidant stress. Circ Res 2000;87:840–4. [PubMed: 11073878]

Camici GG, et al. Genetic deletion of p66(Shc) adaptor protein prevents hyperglycemia-induced endothelial dysfunction and oxidative stress. Proc Natl Acad Sci U S A 2007;104:5217–22. [PubMed: 17360381]

Ceriello A. New Insights on Oxidative Stress and Diabetic Complications May Lead to a “Causal” Antioxidant Therapy. Diabetes Care 2003;26:1589–1596. [PubMed: 12716823]

Chen B, Deen WM. Analysis of the effects of cell spacing and liquid depth on nitric oxide and its oxidation products in cell cultures. Chem Res Toxicol 2001;14:135–47. [PubMed: 11170517]

Chen B, et al. Diffusion and reaction of nitric oxide in suspension cell cultures. Biophys J 1998;75:745–54. [PubMed: 9675176]

Chen K, Popel AS. Theoretical analysis of biochemical pathways of nitric oxide release from vascular endothelial cells. Free Radic Biol Med 2006;41:668–80. [PubMed: 16864000]

Cosentino F, et al. Final common molecular pathways of aging and cardiovascular disease: role of the p66Shc protein. Arterioscler Thromb Vasc Biol 2008;28:622–8. [PubMed: 18162611]

Cosentino F, et al. High glucose increases nitric oxide synthase expression and superoxide anion generation in human aortic endothelial cells. Circulation 1997;96:25–8. [PubMed: 9236411]

Di Filippo C, et al. M40403 prevents myocardial injury induced by acute hyperglycaemia in perfused rat heart. Eur J Pharmacol 2004;497:65–74. [PubMed: 15321736]

Didion SP, et al. Increased superoxide and vascular dysfunction in CuZnSOD-deficient mice. Circ Res 2002;91:938–44. [PubMed: 12433839]

Du X, et al. Inhibition of GAPDH activity by poly(ADP-ribose) polymerase activates three major pathways of hyperglycemic damage in endothelial cells. J Clin Invest 2003;112:1049–57. [PubMed: 14523042]

Economides PA, et al. The effect of vitamin E on endothelial function of micro- and macrocirculation and left ventricular function in type 1 and type 2 diabetic patients. Diabetes 2005;54:204–11. [PubMed: 15616030]

Faraci FM. Vascular protection. Stroke 2003;34:327–9. [PubMed: 12574525]

Fennell JP, et al. Adenovirus-mediated overexpression of extracellular superoxide dismutase improves endothelial dysfunction in a rat model of hypertension. Gene Ther 2002;9:110–7. [PubMed: 11857069]

Fridovich I. Superoxide radical and superoxide dismutases. Annu Rev Biochem 1995;64:97–112. [PubMed: 7574505]

Furchgott RF, Jothianandan D. Endothelium-dependent and -independent vasodilation involving cyclic GMP: relaxation induced by nitric oxide, carbon monoxide and light. Blood Vessels 1991;28:52–61. [PubMed: 1848126]

Garcia Soriano F, et al. Diabetic endothelial dysfunction: the role of poly(ADP-ribose) polymerase activation. Nat Med 2001;7:108–13. [PubMed: 11135624]

Giardino I, et al. BCL-2 expression or antioxidants prevent hyperglycemia-induced formation of intracellular advanced glycation endproducts in bovine endothelial cells. J Clin Invest 1996;97:1422–8. [PubMed: 8617874]

Giugliano D, et al. Diabetes mellitus, hypertension, and cardiovascular disease: which role for oxidative stress? Metabolism 1995;44:363–8. [PubMed: 7885282]

Gladwin MT, Kim-Shapiro DB. The functional nitrite reductase activity of the hemeglobins. Blood 2008;112:2636–47. [PubMed: 18596228]

Gotoh N, Niki E. Rates of interactions of superoxide with vitamin E, vitamin C and related compounds as measured by chemiluminescence. Biochim Biophys Acta 1992;1115:201–7. [PubMed: 1310874]

Graier WF, et al. High D-glucose-induced changes in endothelial Ca2+/EDRF signaling are due to generation of superoxide anions. Diabetes 1996;45:1386–95. [PubMed: 8826976]

Guerci B, et al. Endothelial dysfunction and type 2 diabetes. Part 2: altered endothelial function and the effects of treatments in type 2 diabetes mellitus. Diabetes Metab 2001;27:436–47. [PubMed: 11547217]

Guzik TJ, et al. Mechanisms of increased vascular superoxide production in human diabetes mellitus: role of NAD(P)H oxidase and endothelial nitric oxide synthase. Circulation 2002a;105:1656–62. [PubMed: 11940543]

Guzik TJ, et al. Nitric oxide modulates superoxide release and peroxynitrite formation in human blood vessels. Hypertension 2002b;39:1088–94. [PubMed: 12052847]

Jones CI 3rd, et al. Endothelial cell respiration is affected by the oxygen tension during shear exposure: role of mitochondrial peroxynitrite. Am J Physiol Cell Physiol 2008;295:C180–91. [PubMed: 18480296]

Jones CI 3rd, et al. Regulation of antioxidants and phase 2 enzymes by shear-induced reactive oxygen species in endothelial cells. Ann Biomed Eng 2007;35:683–93. [PubMed: 17340195]

Kavdia M. A computational model for free radicals transport in the microcirculation. Antioxid Redox Signal 2006;8:1103–11. [PubMed: 16910758]

Kavdia M, Popel AS. Wall shear stress differentially affects NO level in arterioles for volume expanders and Hb-based O2 carriers. Microvasc Res 2003;66:49–58. [PubMed: 12826074]

Kavdia M, Popel AS. Venular endothelium-derived NO can affect paired arteriole: a computational model. Am J Physiol Heart Circ Physiol 2006;290:H716–23. [PubMed: 16155098]

Kavdia M, et al. Nitric oxide, superoxide, and peroxynitrite effects on the insulin secretion and viability of betaTC3 cells. Ann Biomed Eng 2000;28:102–9. [PubMed: 10645793]

Kinlay S, et al. Long-term effect of combined vitamins E and C on coronary and peripheral endothelial function. J Am Coll Cardiol 2004;43:629–34. [PubMed: 14975474]

Kojda G, Harrison D. Interactions between NO and reactive oxygen species: pathophysiological importance in atherosclerosis, hypertension, diabetes and heart failure. Cardiovasc Res 1999;43:562–71. [PubMed: 10690328]

Koppenol WH, et al. Peroxynitrite, a cloaked oxidant formed by nitric oxide and superoxide. Chem Res Toxicol 1992;5:834–42. [PubMed: 1336991]

Lamkin-Kennard K, et al. Modeling the regulation of oxygen consumption by nitric oxide. Adv Exp Med Biol 2003;510:145–9. [PubMed: 12580419]

Lash JM, et al. Acute hyperglycemia depresses arteriolar NO formation in skeletal muscle. Am J Physiol 1999;277:H1513–20. [PubMed: 10516190]

Lewis RS, Deen WM. Kinetics of the reaction of nitric oxide with oxygen in aqueous solutions. Chem Res Toxicol 1994;7:568–74. [PubMed: 7981422]

Lewis RS, et al. Kinetic analysis of the fate of nitric oxide synthesized by macrophages in vitro. J Biol Chem 1995;270:29350–5. [PubMed: 7493969]

Lynch SM, et al. Vascular superoxide dismutase deficiency impairs endothelial vasodilator function through direct inactivation of nitric oxide and increased lipid peroxidation. Arterioscler Thromb Vasc Biol 1997;17:2975–81. [PubMed: 9409284]

Maczewski M, et al. Endothelial protection from reperfusion injury by ischemic preconditioning and diazoxide involves a SOD-like anti-O2-mechanism. J Physiol Pharmacol 2004;55:537–50. [PubMed: 15381825]

Marwali MR, et al. Modulation of ADP-induced platelet activation by aspirin and pravastatin: role of lectin-like oxidized low-density lipoprotein receptor-1, nitric oxide, oxidative stress, and inside-out integrin signaling. J Pharmacol Exp Ther 2007;322:1324–32. [PubMed: 17538005]

Moncada S, et al. Nitric oxide: physiology, pathophysiology, and pharmacology. Pharmacol Rev 1991;43:109–142. [PubMed: 1852778]

Nalwaya N, Deen WM. Nitric oxide, oxygen, and superoxide formation and consumption in macrophage cultures. Chem Res Toxicol 2005;18:486–93. [PubMed: 15777088]

Neunteufl T, et al. Effects of vitamin E on chronic and acute endothelial dysfunction in smokers. J Am Coll Cardiol 2000;35:277–83. [PubMed: 10676670]

Nishikawa T, et al. Normalizing mitochondrial superoxide production blocks three pathways of hyperglycaemic damage. Nature 2000;404:787–90. [PubMed: 10783895]

Ozuyaman B, et al. RBC NOS: regulatory mechanisms and therapeutic aspects. Trends Mol Med 2008;14:314–22. [PubMed: 18539530]

Pfeiffer S, et al. Metabolic fate of peroxynitrite in aqueous solution. Reaction with nitric oxide and pH-dependent decomposition to nitrite and oxygen in a 2:1 stoichiometry. J Biol Chem 1997;272:3465–70. [PubMed: 9013592]

Quijano C, et al. Enhanced mitochondrial superoxide in hyperglycemic endothelial cells: direct measurements and formation of hydrogen peroxide and peroxynitrite. Am J Physiol Heart Circ Physiol 2007;293:H3404–14. [PubMed: 17906108]

Radi R. Peroxynitrite reactions and diffusion in biology. Chem Res Toxicol 1998;11:720–1. [PubMed: 9671533]

Rieger JM, et al. Ischemia-reperfusion injury of retinal endothelium by cyclooxygenase- and xanthine oxidase-derived superoxide. Exp Eye Res 2002;74:493–501. [PubMed: 12076093]

Stralin P, Marklund SL. Vasoactive factors and growth factors alter vascular smooth muscle cell EC-SOD expression. Am J Physiol Heart Circ Physiol 2001;281:H1621–9. [PubMed: 11557552]

Takahama U, et al. Thiocyanate cannot inhibit the formation of reactive nitrogen species in the human oral cavity in the presence of high concentrations of nitrite: detection of reactive nitrogen species with 4,5-diaminofluorescein. Chem Res Toxicol 2006;19:1066–73. [PubMed: 16918246]

Title LM, et al. Oral glucose loading acutely attenuates endothelium-dependent vasodilation in healthy adults without diabetes: an effect prevented by vitamins C and E. J Am Coll Cardiol 2000;36:2185–91. [PubMed: 11127459]

Ulker S, et al. Antioxidant vitamins C and E ameliorate hyperglycaemia-induced oxidative stress in coronary endothelial cells. Diabetes Obes Metab 2004;6:442–51. [PubMed: 15479220]

Uppu RM, et al. Acceleration of peroxynitrite oxidations by carbon dioxide. Arch Biochem Biophys 1996;327:335–43. [PubMed: 8619624]

Vaughn MW, et al. Effective diffusion distance of nitric oxide in the microcirculation. Am J Physiol 1998;274:H1705–14. [PubMed: 9612383]

Warnholtz A, et al. Increased NADH-oxidase-mediated superoxide production in the early stages of atherosclerosis: evidence for involvement of the renin-angiotensin system. Circulation 1999;99:2027–33. [PubMed: 10209008]

Weidig P, et al. High glucose mediates pro-oxidant and antioxidant enzyme activities in coronary endothelial cells. Diabetes Obes Metab 2004;6:432–41. [PubMed: 15479219]

Williamson JR, et al. Hyperglycemic pseudohypoxia and diabetic complications. Diabetes 1993;42:801–13. [PubMed: 8495803]

Yang Y, et al. Dynamics of nitric oxide and peroxynitrite during global brain ischemia/reperfusion in rat hippocampus: NO-sensor measurement and modeling study. Neurochem Res 2008;33:73–80. [PubMed: 17674204]

Zhang J, et al. Comparison of protective effects of aspirin, D-penicillamine and vitamin E against high glucose-mediated toxicity in cultured endothelial cells. Biochim Biophys Acta 2006;1762:551–7. [PubMed: 16624537]

Zielonka J, et al. Detection of 2-hydroxyethidium in cellular systems: a unique marker product of superoxide and hydroethidine. Nat Protoc 2008;3:8–21. [PubMed: 18193017]

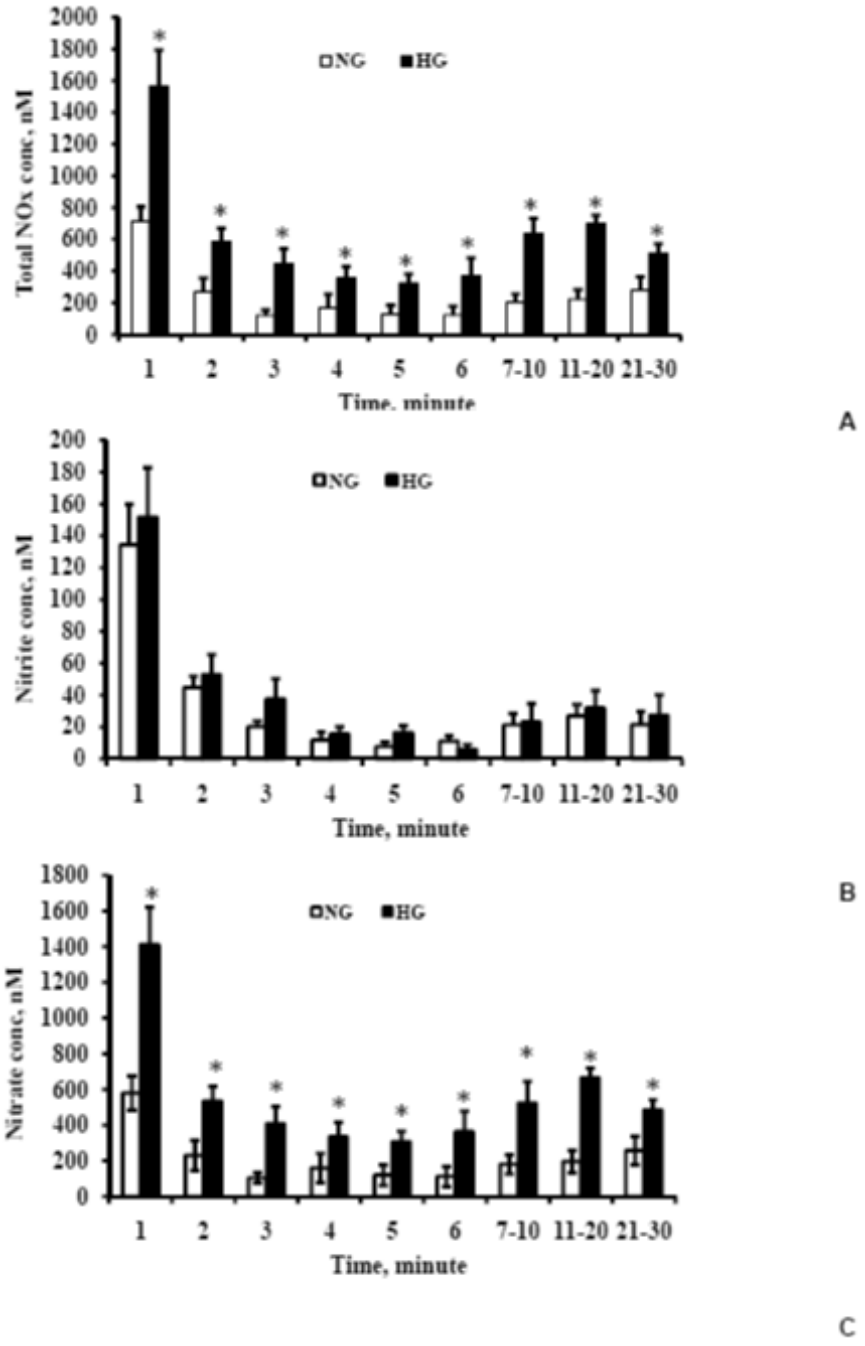

Figure 1A-C. Total NOx, nitrite and nitrate concentrations, respectively in the exiting media
NG represents normal glucose (1000 mg/L) and HG represents high glucose (4500 mg/L). Total NOx and nitrate concentrations were significantly higher in high glucose-exposed endothelial cells indicating a higher production of NO. Values are means ± SE. *Indicates significant difference in the concentration with $p<0.05$ versus corresponding values for normal glucose treatment.

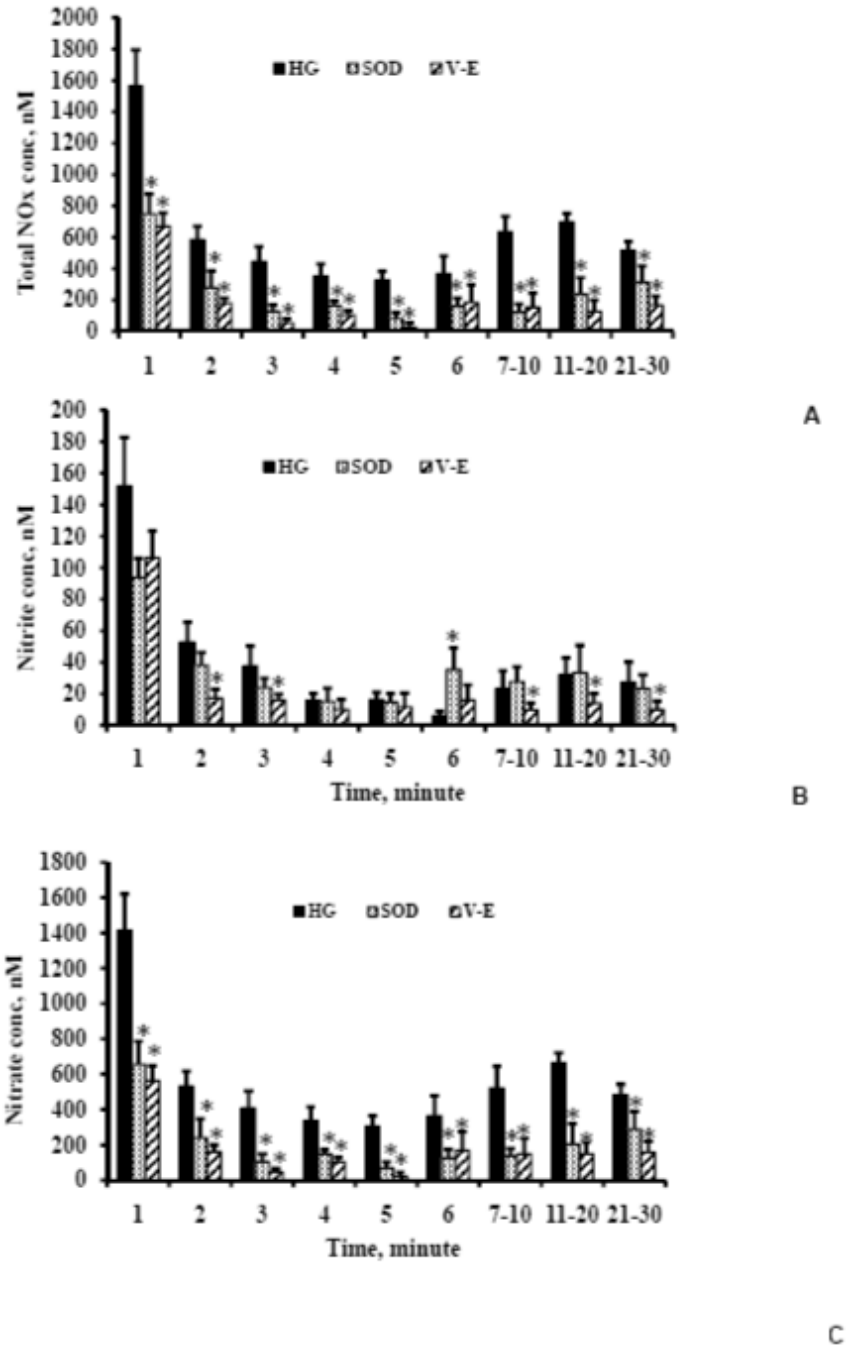

Figure 2A-C. Total NOx, nitrite and nitrate concentrations, respectively in high glucose (4500 mg/L), high glucose with 100 U/ml SOD and high glucose with 100 μM α-tocopherol

The total NOx and nitrate concentrations significantly reduced in SOD or α-tocopherol as compared to that of in high glucose. Also, the nitrite concentrations were significantly lower for most of the time points in α-tocopherol as compared to that of in high glucose. n=4 for SOD and α-tocopherol. Values are mean ± SE. * Indicates significant difference in concentrations with $p<0.05$ versus corresponding values for high glucose.

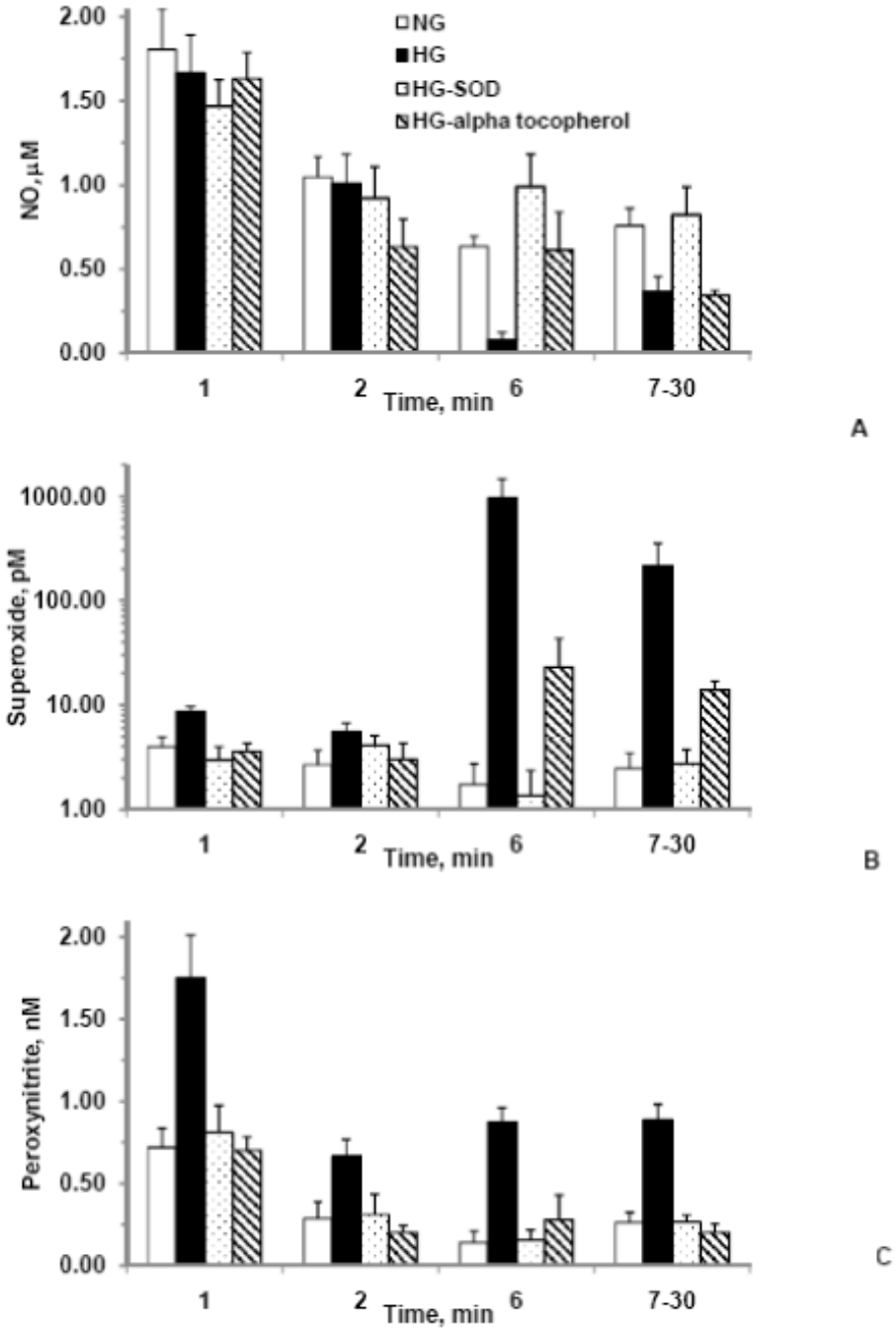

Figure 3A-C. Predicted concentrations of nitric oxide, superoxide, and peroxynitrite, respectively for normal glucose (1000 mg/L) (NG), high glucose (4500 mg/L) (HG), high glucose with 100 U/ml SOD (HG-SOD), and high glucose with 100 μM α-tocopherol (HG-alpha-tocopherol)

The concentrations were obtained using the mathematical model developed on the basis of individual values of nitrite and nitrate productions and reaction kinetics for NO and O_2^-. Superoxide concentrations were much higher in the high glucose whereas NO concentrations were much lower in the high glucose as compared to that of in the normal glucose. The model predicted reduction in O_2^- concentrations and improvement in NO concentrations in SOD as compared to that of in the high glucose. However, NO concentrations were lower in the α-tocopherol as compared to that of in the high glucose. Values are mean ± SE.

Table 1
Dynamics of endothelial cell NO and O_2^- production

NO production, pmol s^{-1} cm^{-2}				
	1 min	2 min	6 min	7-30 min
Normal glucose	1.19±0.15	0.45±0.14	0.20±0.09	0.39±0.11
High glucose	2.61±0.38	0.98±0.13	0.61±0.18	1.02±0.11
α-tocopherol	1.12±0.14	0.30±0.05	0.30±0.19	0.28±0.09
SOD	1.24±0.20	0.46±0.17	0.27±0.08	0.37±0.14
Superoxide production, pmol s^{-1} cm^{-2}				
	1 min	2 min	6 min	7-30 min
Normal glucose	0.97±0.16	0.39±0.14	0.26±0.12	0.43±0.11
High glucose	2.37±0.35	0.89±0.14	1.90±0.29	1.72±0.30
α-tocopherol	0.95±0.11	0.27±0.05	0.37±0.20	0.28±0.06
SOD	1.32±0.27	0.60±0.26	0.27±0.10	0.48±0.08